Available online at www.sciencedirect.com
ScienceDirect
Journal of Photochemistry and Photobiology A: Chemistry 183 (2006) 315–321
Journal of Photochemistry and Photobiology A:Chemistry
www.elsevier.com/locate/jphotochem

Close-conjugation of quantum dots and gold nanoparticles to sidewall functionalized single-walled carbon nanotube templates

Vasudevanpillai Biju [a,*], Tamitake Itoh [a], Yoji Makita [b], Mitsuru Ishikawa [a]

[a] *Nano-Bioanalysis Team, Health Technology Research Center (HTRC), National Institute of Advanced Industrial Science and Technology (AIST), 2217-14 Hayashi-cho, Takamatsu, Kagawa 761-0395, Japan*

[b] *Health Hazard Reduction Team, Health Technology Research Center (HTRC), National Institute of Advanced Industrial Science and Technology (AIST), 2217-14 Hayashi-cho, Takamatsu, Kagawa 761-0395, Japan*

Available online 5 July 2006

Abstract

Two types of nanoscale hybrid materials have been synthesized by conjugating CdSe–ZnS quantum dots (QDs) and gold nanoparticles (NPs) to sidewall functionalized single-walled carbon nanotube (SWNT) templates, and examined photoluminescence (PL) properties of the hybrid materials. The two types of hybrid nanoscale materials are SWNT–QD and SWNT–gold–NP conjugates. Excessive sidewall functionalization of SWNT into nitro- and amino-derivatives provided weak PL and water solubility to the SWNT derivatives. Solubility of SWNT derivatives in aqueous media was helpful for efficient conjugation of SWNTs to QDs and gold–NPs. The SWNT–QD and SWNT–gold–NP conjugates were characterized using atomic force microscopy (AFM) imaging. From AFM imaging we identified that the sidewall functionalized SWNTs assisted the formation of one-dimensional close-conjugates of QDs and gold–NPs. Although the nitro- and amino-derivatives of SWNT showed weak PL, conjugation of gold–NPs to the amino-derivative quenched the PL quantitatively. On the other hand, conjugation of luminescent QDs to SWNTs resulted in a partial (∼35%) quenching of PL from QDs. We attributed the quenching of PL from SWNTs by gold–NPs to non-radiative energy transfer between SWNTs and gold–NPs or vice versa, and the quenching of PL from QDs is due to non-radiative energy transfer from QDs to SWNTs. In the current work, we demonstrated a simple method of close-packing of QDs and gold–NPs using functionalized SWNT templates. Also, we identified that PL properties of SWNTs and QDs are affected in the close-packed structures. SWNT and NP based hybrid materials show great promise as building blocks for nanoscale devices. In this regard the preparation and understanding of the properties of SWNT–QD and SWNT–gold–NP conjugates would be useful during the design of various hybrid nanoscale materials for device applications.

Keywords: Quantum dots; Nanoparticles; Single-walled carbon nanotube; Photoluminescence; Gold; CdSe–ZnS; SWNT

1. Introduction

Nanoparticles (NPs) and nanotubes are promising materials for developing nanoscale opto-electronic devices. Among different nanoscale materials semiconductor quantum dots (QDs), metal NPs, and carbon nanotubes (CNTs) are interesting for their structure, unique physical properties, and emerging applications in different fields. Specifically, size tuneable band gaps, bright and stable photoluminescence (PL), and wide absorption and narrow emission bands [1–4] make QDs promising materials for applications in nanotechnology and biological imaging. The rigid one-dimensional structure, metallic to semiconducting properties, and doping induced band-gap tailoring of CNTs are promising for developing nanoscale electronic devices such as transistors [5–8]. In addition to the fundamentally interesting properties of CNTs and QDs, conjugations of metal and semiconductor NPs to CNTs are expected to provide: (1) novel hybrid nanoscale materials, and (2) advanced optical, electronic, and mechanical properties to nanoscale hybrid systems.

Structural modification of CNTs by conjugation to various organic [9–13], biological [14,15], and inorganic [16–20] materials has been found to be a versatile method for developing CNT based nanoscale hybrid materials; however, structure–function relations of such materials are still under investigation. Different covalent and non-covalent conjugation methods recently becomes available for interfacing organic molecules, biomaterials, and inorganic NPs to single-walled CNTs (SWNTs) and multi-walled CNTs (MWNTs). For non-covalent conjugations, various methods including π-stacking of poly aromatic hydrocarbons [21], and wrapping in hydrophobic pockets of molecules

* Corresponding author. Tel.: +81 87 869 3558; fax: +81 87 869 4113.
E-mail address: v.biju@aist.go.jp (V. Biju).

1010-6030/$ – see front matter © 2006 Elsevier B.V. All rights reserved.
doi:10.1016/j.jphotochem.2006.06.032

such as polymers and DNA [22–24] were recently used. For covalent conjugations, reactions such as cycloadditions [13], radical additions [9,10,13], and oxidation [11–16] are standard methods. Introduction of carboxylic groups at the ends of CNTs by acid oxidation [11–16] is a powerful method for integrating CNTs to other molecular systems and devices. One of the advantages of the end oxidation methods is that the electronic properties of CNTs are not considerably affected due to oxidation. Nonetheless, sidewall functionalization of CNTs can disorder the π-conjugated lattice structure and is likely to provide poor electronic and mechanical properties to CNTs. However, for applying CNTs as templates for assembling other materials such as QDs and metal NPs, sidewall functionalization is a useful method [18–20]. In the current work, we selected a known procedure for sidewall functionalization of SWNT [9,10], and used the functionalized SWNTs for fabricating arrays of QDs and gold–NPs. We identified that QDs can be linearly arranged by using sidewall functionalized SWNT templates; the structural rigidity of SWNT was not completely retained due to excessive sidewall reaction though. Also, from ensemble averaged PL measurements we identified that conjugation of QDs and gold–NPs to SWNT reduce the PL intensities of QDs and SWNTs, respectively. The reduced PL intensities of QDs and SWNTs are attributed to non-radiative energy transfer processes.

2. Experimental

2.1. Materials

The core materials used in the current work are streptavidin conjugated CdSe–ZnS QDs (Quantum Dot Corporation, Hayward, CA), gold–NPs (Funakoshi, Tokyo), and SWNT (Aldrich, Tokyo). Reagent grade sodium dodecyl sulfate (SDS, Aldrich, Tokyo), 4-nitrobenzenediazonium tetrafluoroborate (Aldrich, Tokyo), biotin *N*-hydroxysuccinimide ester (biotin-NHS-ester, Sigma, Tokyo), and sodium borohydride ($NaBH_4$, Aldrich, Tokyo) were used for preparing nitro-, amino-, and biotin-functionalized SWNTs. Mercaptoacetic acid (Aldrich, Tokyo) was used for surface modification of gold–NPs. Spectroscopic grade dimethyl sulfoxide (DMSO, Wako, Tokyo), and Milli Q water (Millipore Corporation, Billerica, MA) were used in chemical reactions and spectral measurements.

2.2. Conjugation of QDs and gold–NPs to SWNT

QDs and gold–NPs were conjugated to sidewall functionalized SWNTs. For sidewall functionalization of SWNT, we selected an addition reaction of a diazonium salt; several other methods including cycloadditions, alkylation, and oxidation are available though. Additions of *p*-substituted phenyl radicals, generated from corresponding diazonium salts, were found to be efficient in sidewall functionalization of SWNT [9,10]. Steps involved in the preparation of SWNT–QD and SWNT–gold–NP conjugates are shown in Scheme 1. Experimental details involved in the preparations are described here. A suspension of SWNT was prepared by dispersing it in an SDS surfactant solution. For this, SDS was dissolved in water (250 mg/25 mL) to form a solution above the critical micelle concentration. This was followed by adding 50 mg of SWNT, and the SDS-SWNT mixture was sonicated for 12 h at room temperature. This procedure provided a black colored aqueous micellar suspension of SWNT. The SWNT suspension was cooled to 10 °C and a cold (10 °C) aqueous solution of *p*-nitrobenzenediazonium tetrafluoroborate (77 mg, 0.3 mmol) was added to it. This reaction mixture was vigorously stirred at 10 °C for 72 h, during which the diazonium salt decomposed into a *p*-nitrophenyl free-radical [10], and the radical reacted at the sidewall of SWNT. The reaction mixture was gradually (over 30 min) warmed to room temperature, excess water was added, and it was filtered under suction. The filtration provided a dark residue, and the *p*-nitrobenzenediazonium tetrafluoroborate left unreacted was removed by repeated washing using methanol (10 mL, five times). The dark residue was likely to contain pristine SWNT and *p*-nitrobenzene adducts of SWNT. Pristine SWNT and less-reacted SWNTs are insoluble or less soluble in DMSO. Therefore, unreacted SWNTs and less-reacted SWNTs were removed by suspending the residue in DMSO (5 mL) followed by a silica-gel filtration using DMSO as eluent. During the silica-gel filtration process unreacted and less-reacted SWNTs were trapped inside the column. This was confirmed from the presence of a trapped dark band in the column and its absorption spectrum. The absorption spectrum of the trapped residue inside the silica-gel showed electronic transition features characteristic to pristine SWNT [9,10]. DMSO was removed from the dark brown solution by distillation under reduced pressure and provided 35 mg of *p*-nitrobenzene functionalized SWNT (nitro-SWNT). The nitro-SWNT showed good solubility in DMSO (>2 mg/mL) and the solution was deep brown in color (photograph 'b' in Fig. 1A) in contrast to the black suspension of pristine SWNT in SDS micelles (photograph 'a' in Fig. 1A).

We reduced the nitro-SWNT into its *p*-aniline derivative (amino-SWNT) using $NaBH_4$ (Scheme 1). Although electrochemical reduction is a known method for converting nitro-SWNT into amino-SWNT, in the current work we selected reduction using $NaBH_4$ for technical reasons. The nitro-SWNT (25 mg) was dissolved in dry DMSO (25 mL), and heated to 160 °C under N_2 atmosphere. The solution was stirred well and $NaBH_4$ (25 mg) was added in five portions into the hot solution of nitro-SWNT over 25 min. The reduction reaction was carried out at 160 °C for 1 h after complete addition of $NaBH_4$. We observed a gradual color change from dark brown to deep yellow during the course of the reduction reaction. After 1 h, the reaction mixture was cooled to room temperature and any $NaBH_4$ left unreacted was decomposed by carefully adding 1 mL of cold water. This was followed by reducing the volume of the solution to ∼5 mL by distillation under reduced pressure. The amino-SWNT was isolated from the reaction mixture by column chromatography using silica-gel and DMSO. DMSO was removed from the eluted solution by distillation under reduced pressure and this provided 20 mg of amino-SWNT. A solution of the amino-SWNT compound (photograph 'c' in Fig. 1A) was distinctly different from that of the nitro-SWNT compound in color and absorption spectrum; the amino-SWNT derivative showed a higher molar extinction coef-

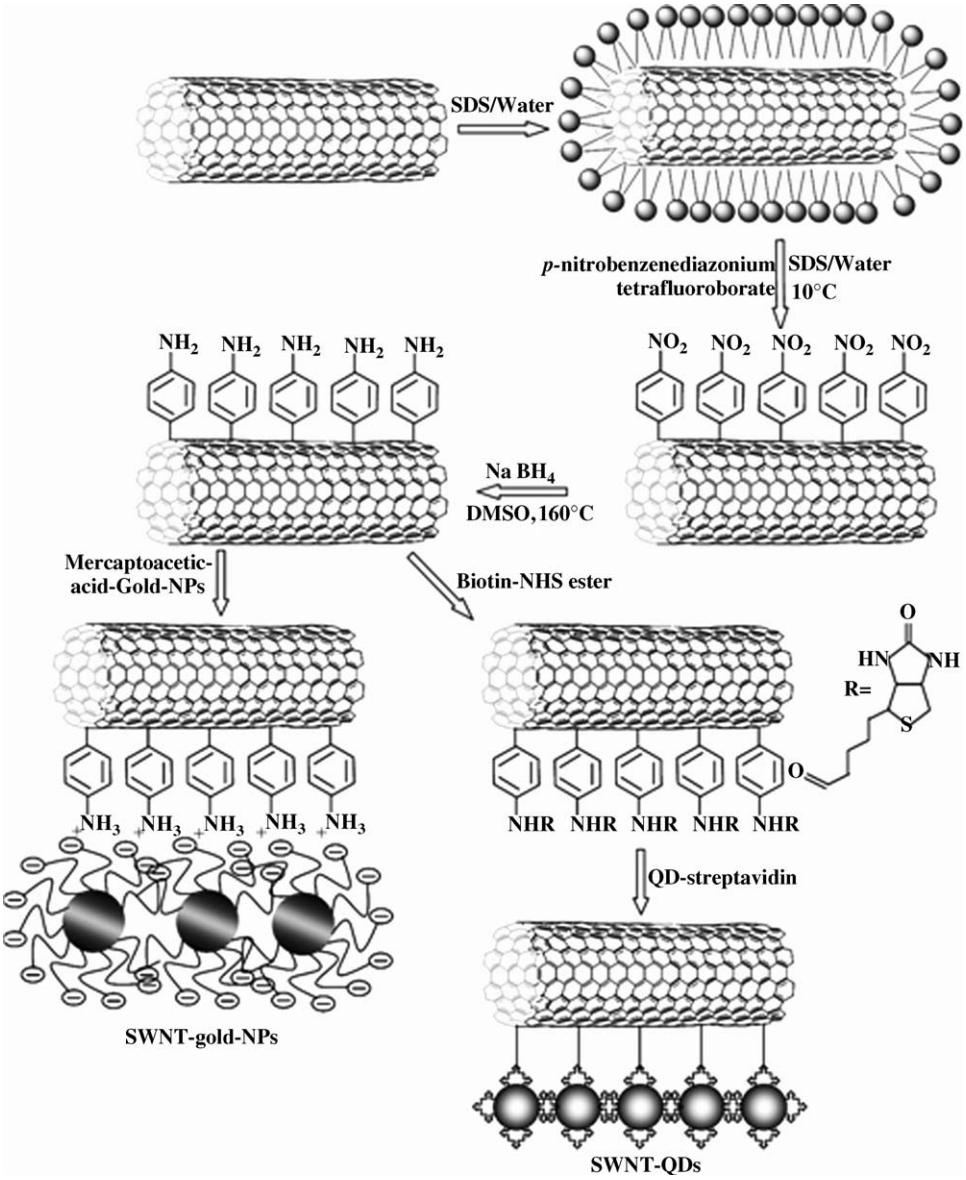

Scheme 1. Steps involved in the functionalization of SWNT and successive conjugation to gold–NPs and streptavidin conjugated QDs.

ficient ~400 nm (trace 'a' in Fig. 1B) compared to that of the nitro-SWNT derivative (trace 'b' in Fig. 1B). The absorption spectra 'a' and 'b' were recorded for 50 μg/mL DMSO solutions of amino-SWNT and nitro-SWNT, respectively. Furthermore, compared to the limited solubility of nitro-SWNT in DMSO, amino-SWNT showed solubility in various solvents including water:DMSO mixtures (containing >10%, v/v DMSO), aqueous buffers (<pH 6), DMSO, and toluene. The solubility of amino-SWNT in acidic buffers is due to the formation of ammonium salts.

The amino-SWNT was conjugated to gold–NPs and QDs through ammonium salt formation and biotin-streptavidin coupling, respectively. For the conjugation of gold–NPs to amino-SWNTs, gold–NPs were reacted with mercaptoacetic acid. This reaction provides gold–NPs with free surface carboxylic acid groups. The carboxylic acid functionalized gold–NPs were purified by repeated centrifugation and mixed with amino-SWNT. Thus, gold–NPs were attached to SWNTs through quaternary ammonium salt formation (Scheme 1). The conjugates of gold–NPs and amino-SWNT was characterized from PL measurements and AFM imaging. For the conjugation of QDs to amino-SWNT, we followed the widely used procedure of streptavidin–biotin coupling reaction (Scheme 1). For this, the amino-SWNT was biotinylated using biotin-NHS-ester. In a typical biotinylation reaction, a solution of amino-SWNT (prepared in a water-DMSO mixture by dissolving 15 mg of amino-SWNT in 5 mL DMSO followed by adding 1 mL water) was reacted with a DMSO solution of biotin–NHS ester (1 mL, 10 mM) for 2 h at room temperature. The reaction mixture was loaded onto a silica-gel column, and the biotin-NHS ester left unreacted was removed by elution using methanol. The biotinylated SWNTs collected at the top of the column, were eluted in a second stage using DMSO. No further purification was carried out to remove amino-SWNT left unreacted considering selective

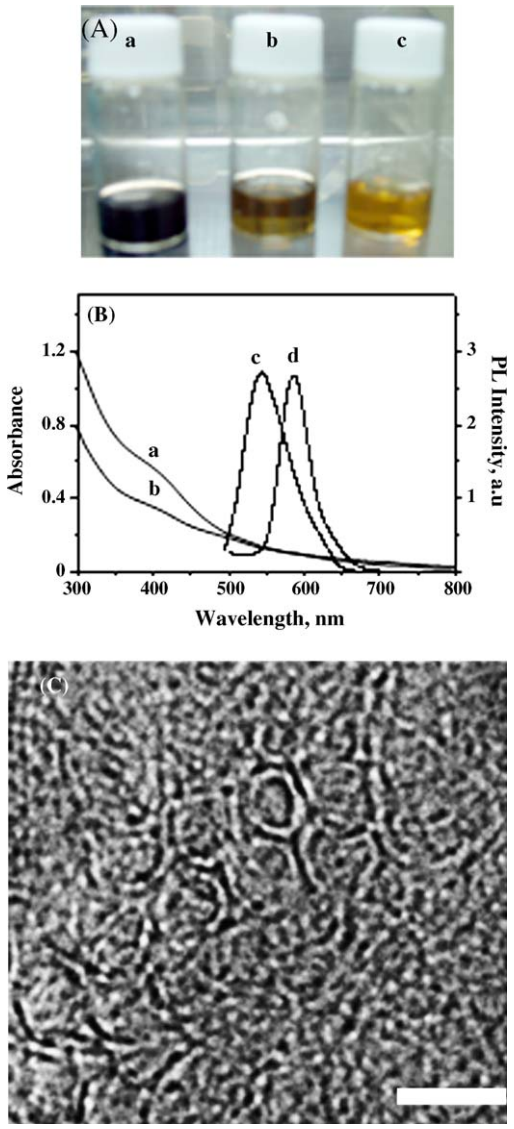

Fig. 1. (A) Photographs of: (a) SWNT dispersed in 1% SDS micelles, (b) nitro-SWNT dissolved in DMSO, and (c) amino-SWNT dissolved in a water:DMSO mixture (9:1, v/v); (B) absorption and normalized PL spectrums of sidewall functionalized SWNTs: (a) absorption spectrum of amino-SWNT (50 μg/mL) in a water:DMSO mixture (9:1, v/v), (b) absorption spectrum of nitro-SWNT (50 μg/mL) in DMSO, (c) PL spectrum of nitro-SWNT in DMSO, and (d) PL spectrum of amino-SWNT in a water:DMSO mixture (9:1, v/v); (C) TEM image of a amino-SWNT sample dispersed on a carbon coated copper grid. Scale bar in (C) is 5 nm.

binding of biotin to streptavidin-conjugated QDs in the next step. Streptavidin conjugated QD (λ_{em} = 605 nm) solution was diluted to a 0.2 μM solution using a specified buffer supplied with the commercial QD sample, and the 0.2 μM solution of QDs was mixed with a solution of biotinylated SWNT (10 μg/L in a 1:9, v/v DMSO:water mixture). The streptavidin–biotin conjugation reaction was allowed for 2 h at room temperature, and the sample was then stored at 4 °C. The conjugation step involving QDs was carried out in the dark to avoid possible photo-darkening of QDs. Formation of SWNT–QD conjugates was identified from fluorescence spectral measurements and AFM imaging.

2.3. Preparation of samples

Samples for atomic force microscopy (AFM) imaging were prepared by spin coating (3000 rpm) aqueous solutions of SWNT–QD and SWNT–gold–NP conjugates on freshly cleaved mica plates. Concentrations of the solutions used for sample preparations were equivalent to 10 μg/L of biotinylated SWNT. Molar concentration of biotinylated SWNT was not determined considering a possible error due to a size distribution of SWNTs and an unknown number of functional groups on SWNTs. Reference samples were prepared from 0.1 nM aqueous solutions of gold–NPs and streptavidin conjugated QDs. Samples for transmission electron microscopy (TEM) imaging were prepared by incubating a DMSO solution (0.1 μg/mL) of amino-SWNTs on carbon coated copper grids, followed by drying under vacuum. The concentrations of samples used in the PL measurements were the same as that in AFM measurements.

2.4. Instruments used

Absorption and emission spectra were recorded using a spectrophotometer (Hitachi U-4100, Hitachi, Tokyo) and a spectrofluorometer (Hitachi F-4500, Hitachi, Tokyo), respectively. AFM images were recorded using an MFP-3D microscope (Asylum Research, Santa Barbara, CA). Tapping-mode AFM images were collected in air using ultra-sharp (radius of curvature <10 nm) Al nanoprobes (Olympus, Tokyo). The cantilevers used were 160 μm long with a spring constant of 42 N/m and a resonance frequency of 300 kHz. TEM images were recorded using a 300 kV JEOL JEM 3010 microscope.

3. Results and discussion

Functionalization of SWNT into nitro- and amino-derivatives was confirmed from UV–vis–NIR absorption and IR spectra. Typical absorption spectra of amino-SWNT and nitro-SWNT solutions in DMSO are shown in Fig. 1B (traces ‘a’ and ‘b’). It is widely known that pristine SWNT in SDS micelles show distinctive absorption spectral features, the so-called van Hove signatures [9,10]. In the current work, nitro-SWNT and amino-SWNT provided structure-less absorption bands extending into the UV–vis–NIR region. Dyke and Tour reported similar structure-less absorption bands for functionalized SWNTs [9,10]. The structure-less absorption bands are attributed to loss of electronic transitions due to sidewall functionalization. Also, functionalized SWNTs (both the nitro- and amino-derivatives) showed weak PL in the visible region. Typical PL spectrums of nitro- and amino-functionalized SWNTs are shown in traces ‘c’ and ‘d’, respectively in Fig. 1B. We observed a red-shifted PL maximum (λ_{max} = 585) and a narrow PL spectral width (fwhm = 47 nm) for the amino-SWNT compared to the nitro-SWNT (λ_{max} = 544, fwhm = 70 nm). The different PL maxima observed for nitro-SWNT and amino-SWNT can be explained in terms of different excitonic energy states induced by functional groups. The red-shifted PL maximum observed for amino-SWNT is probably due to an increased electron density contributed by the aniline group we consider that overlapping electronic states of the ani-

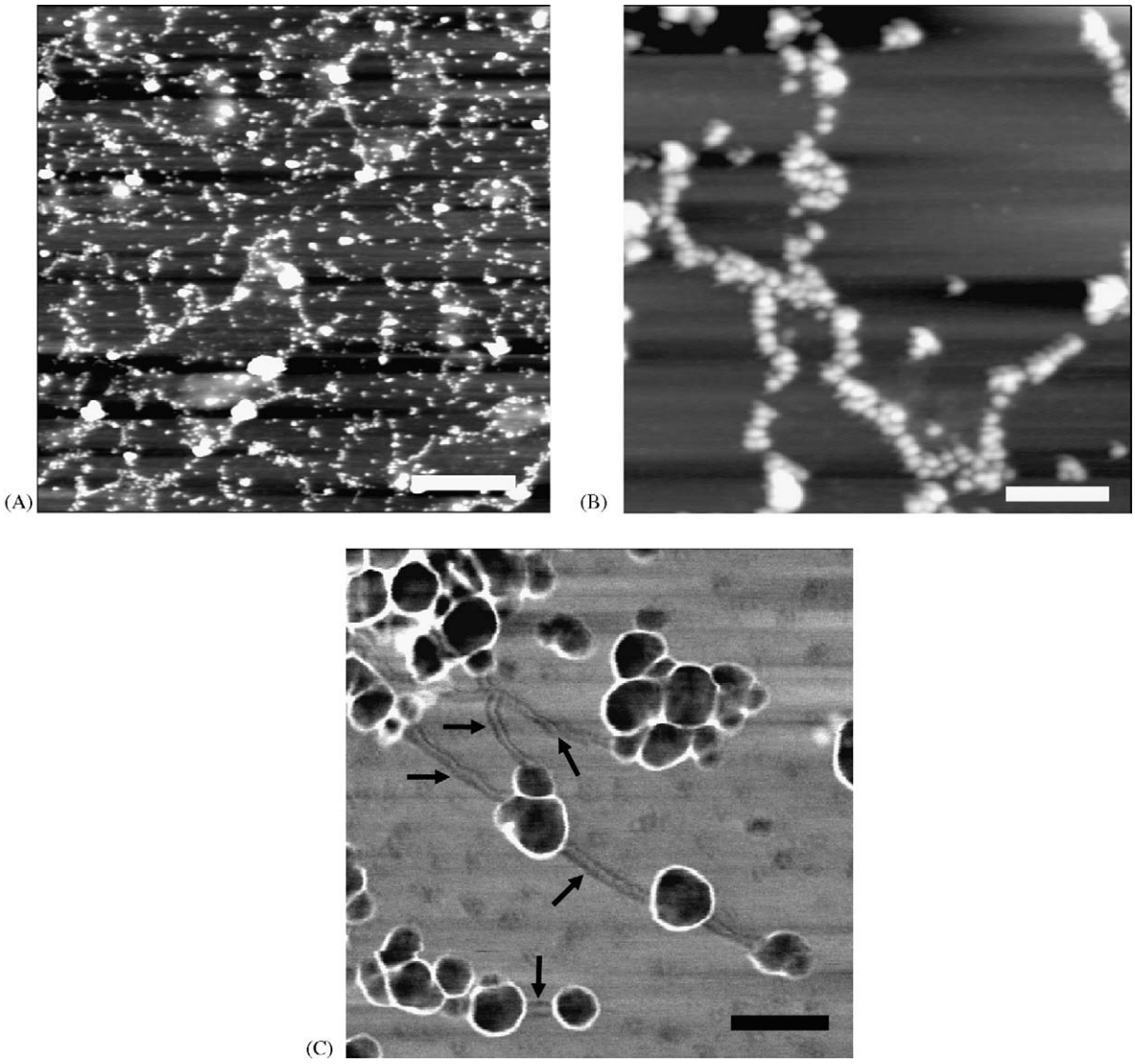

Fig. 2. (A) Tapping mode AFM height image of SWNT–QD conjugates dispersed on a mica plate; (B) high-resolution AFM height image of SWNT–QD conjugates dispersed on a mica plate; (C) AFM phase image of SWNT–gold–NPs conjugates dispersed on a mica plate. The arrows in (C) locate bare SWNTs. Scale bars in (A)–(C) are 2 μm, 500 nm, and 50 nm, respectively.

line moiety with the electronic envelop of SWNT increases the stability of the excited states of the amino-SWNT derivative. On the other hand, nitrobenzene has an electron withdrawing effect, which in-turn probably cannot stabilize excitons in nitro-SWNT derivatives. Indeed, we are unable to identify a definitive reason for the different PL spectral widths observed for nitro-SWNT and amino-SWNT.

In addition to examining the absorption and PL spectra of functionalized SWNTs, we examined the structures of functionalized SWNTs using TEM imaging and compared the structures with that of pristine SWNT. A typical TEM image of an amino-SWNT sample is shown in Fig. 1C. From the TEM images, we identified that functionalized SWNTs have flexible structures. In contrast to the long-range rigid structure of pristine SWNT, we noticed large structural flexibility even within 5 nm for amino-SWNT and nitro-SWNT. However, such large flexibility within a short length was not observed for nitro-SWNT in a previous investigation [10]. We attributed the flexible structures of the functionalized SWNTs in the current work to excessive sidewall reactions under prolonged treatments. In short, introduction of a large number of functional groups via addition reactions at several double bonds on the SWNT surface probably resulted in a partial loss of structural rigidity of SWNTs in the current work.

The structures of SWNT–QD and SWNT–gold–NP hybrid nanoscale materials were examined using tapping mode AFM imaging in air. Typical AFM images of SWNT–QD and SWNT–gold–NP are shown in Fig. 2A and C, respectively. We identified that conjugation of QDs to biotinylated SWNT produced close-packed one-dimensional QD assemblies, extending from a few hundred nanometers to several microns. The presence of SWNT–QDs having different lengths is probably due to a size distribution of SWNTs in commercial sample. Another possibility that linear extension of biotinylated SWNTs through streptavidin bridging is unlikely in the current work. If leaner bridging of biotinylated SWNTs is possible through multiple streptavidin molecules present on the surface of individual QDs,

lateral extension is also possible. However, under the selected concentrations for the preparation of SWNT–QD conjugates, we are unable to identify lateral extension of SWNT–QD structures. Therefore, linear extension of the structures is also difficult to be discussed in terms of multiple-biotin binding of streptavidin-QDs. From a close examination of AFM images of SWNT–QD conjugates, we identified that QDs are linearly close-packed on biotinylated SWNT templates. A high resolution AFM image of a linear assembly of SWNT–QDs is shown in Fig. 2B. The linear close-packing of streptavidin-linked QDs is due to the high degree sidewall functionalization of SWNT and strong binding of biotin to streptavidin. The possibility that self-association of streptavidin coated QDs into linear structures was ruled out on the basis of the observation of isolated QDs and small clusters (∼50 nm) in AFM images in the absence of biotinylated SWNT.

In contrast to the formation of close-packed QDs on biotinylated SWNT templates, we identified that only a small number of gold–NPs are attached to amino-SWNTs. From AFM imaging, we found that a large number of clusters of gold–NPs are present in SWNT–gold–NP samples. A low-density conjugation of gold–NPs on SWNTs is identified from AFM imaging (Fig. 2C). The low density conjugation of gold–NPs on SWNTs is due to a weak interaction between the amino-groups on the side wall of SWNT and the carboxylic groups on the surface of gold–NPs compared to a strong streptavidin–biotin binding in the case of SWNT–QD conjugates. This observation indicated that amine-carboxylic acid coupling via quaternary ammonium salt formation is less efficient for the preparation of hierarchical nanostructures such as SWNT–QD conjugates. Although the density of gold–NPs on SWNTs was not well controlled, the current work demonstrated the preparation of hybrid nanoscale structures involving potentially important material such as SWNT, QDs, and gold–NPs. Furthermore, the conjugations of QDs and gold–NPs to SWNT templates are likely to induce electronic interactions between the components and perturb the energy states of each other.

From absorption and PL spectra we identified electronic interactions of SWNT with QDs and gold–NPs in SWNT–QD and SWNT–gold–NP conjugates. Typical PL spectra of QDs before (trace 'a') and after (trace 'b') conjugation to biotinylated SWNT are shown in Fig. 3A; a correction was included in spectrum 'b' to compensate absorbance of biotinylated SWNT. The conjugation of QDs to SWNT resulted in a partial (35%) quenching of PL intensity of QDs. This quenching of the PL intensity was not due to non-specific interactions between QDs and SWNT. This was confirmed from PL measurements of QDs in the presence of non-biotinylated SWNTs. In the presence of non-biotinylated SWNT, quenching of PL was not significant. We considered two possibilities for the quenching of the PL intensity of QDs: (1) Förster resonance energy transfer (FRET) from smaller to bigger QDs [25] in close-packed SWNT–QD structures, and (2) FRET from QD to SWNT. Detailed investigations involving multiplexing of QDs having different size on the same SWNT template and preparation of SWNT–QD conjugates having different densities of QDs are underway in our laboratory to identify the origin of the PL intensity quenching of QDs.

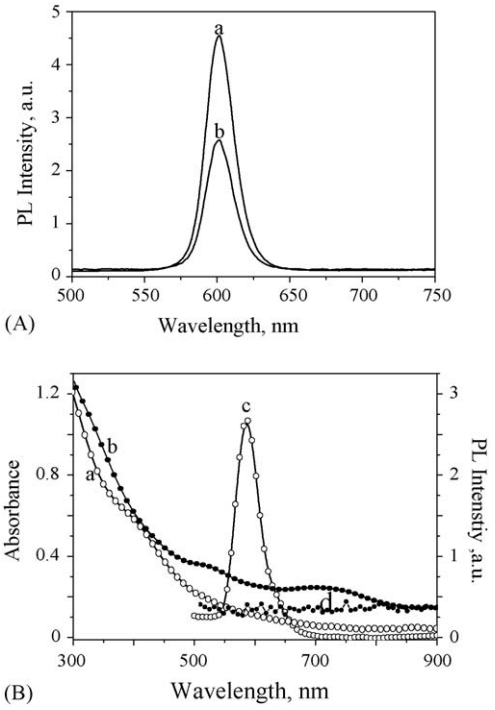

Fig. 3. (A) PL spectrums of streptavidin conjugated QDs (a) and SWNT–QD conjugates (b). Equal amounts of QDs were involved in both the measurements, and a correction was included in spectrum 'b' to account for the absorbance of SWNT. The samples were excited at 450 nm. (B) Absorption and emission spectrums of SWNT conjugates: (a) absorption spectrum of amino-SWNT, (b) absorption spectrum of SWNT–gold–NP conjugates, (c) PL spectrum of amino-SWNT, and (d) PL spectrum of SWNT–gold–NP conjugates.

In contrast to the partial quenching of the PL intensity of QDs in SWNT–QD conjugates, conjugation of gold–NPs to amino-SWNT resulted in a quantitative quenching of PL from SWNTs. PL spectra of SWNT before and after conjugation to gold–NPs are shown in traces 'c' and 'd', respectively in Fig. 3B. In addition to the quenching of PL from SWNTs by gold–NPs, we observed a weak red-shifted band (∼730 nm) in the absorption spectrum (trace 'b' in Fig. 3B) of SWNT–gold–NP conjugates. Although the quenching of PL in SWNT–QD (quenching of QD's PL) and SWNT–gold–NPs (quenching of SWNT's PL) conjugates are different, energy transfer is likely to be a common mechanism of PL quenching in the SWNT–NP systems. Conjugation of fluorescent molecules to metal NPs is known to quench or enhance the fluorescence emission intensity due to energy transfer. The efficient quenching of PL from SWNTs observed in the current work indicates that the gold–NPs are closely conjugated to SWNTs. Also, the close-conjugation of gold–NPs to SWNTs probably induced a weak charge transfer interaction between SWNT and gold–NPs. We attributed the weak absorption band ∼730 nm to charge transfer interaction between SWNT and gold–NPs. Yet another possibility, the long wavelength absorption band is a plasmon band of linear arrays of gold–NPs on SWNT is also not ruled out. We observed that the band ∼730 nm disappeared upon changing the pH of a SWNT–gold–NP conjugate solution to 8 or higher. The disappearance of the charge transfer band is probably due to dissociation of the quaternary ammonium salt under basic

pH. A detailed investigation related to the particle plasmon, the structure of SWNT–gold–NP conjugates, the quenching of PL, and literature reports is necessary for further understanding of the optical properties of SWNT–gold–NP conjugates.

4. Conclusions

We employed sidewall functionalization of SWNT to prepare hierarchical nanoscale hybrid materials such as SWNT–QD and SWNT–gold–NP conjugates. Excessive sidewall functionalization of SWNT under a prolonged reaction was helpful for preparing water-soluble derivatives of SWNT. We identified that the structural rigidity of SWNT was not completely retained after excessive sidewall functionalization. A combination of the high solubility of the functionalized SWNT in aqueous medium and the presence functional groups such as biotin and amine made SWNT an ideal template for linear close-conjugation of QDs and gold–NPs. From the absorption and PL spectral measurements we obtained indications that conjugation of QDs and gold–NPs to SWNT induces charge transfer and non-radiative energy transfer interactions between the components. These interactions perturbed their energy states, and absorption and PL characteristics. Rather than a specific method for the preparation of QD and gold–NP conjugated SWNTs, the current work demonstrated: (1) the use of potentially important nanomaterials such as QDs, gold–NPs, and SWNT for fabricating hybrid nanoscale materials, and (2) the effect of interfacing nanomaterials on their photophysical properties. We believe that hierarchical nanoscale hybrid structures based on the above materials and an understanding of their optical properties would be promising during construction of light harvesting systems [26,27] and nanoscale optoelectronic devices.

Acknowledgement

VB and MI are grateful to the Grant-in-Aid for Scientific Research (KAKENHI-17034068) in Priority Area “Molecular Nano Dynamics” from the Ministry of Education, Science, and Culture, Japan.

References

[1] A.P. Alivisatos, Science 271 (1996) 933–937.
[2] C.B. Murray, C.R. Kagan, M.G. Bawendi, Annu. Rev. Mater. Sci. 30 (2000) 545–610.
[3] M. Nirmal, L.E. Brus, Acc. Chem. Res. 32 (1999) 407–414.
[4] W.C.W. Chan, S.M. Nie, Science 281 (1998) 2016–2018.
[5] S. Ijima, Nature 354 (1991) 56–58.
[6] P.M. Ajayan, Chem. Rev. 99 (1999) 1787–1800.
[7] M.S. Dresselhaus, G. Dresselhaus, Ph. Avouris, Carbon Nanotubes: Synthesis, Structure, Properties and Applications, Springer, Berlin, 2001.
[8] H. Dai, Acc. Chem. Res. 35 (2002) 1035–1044.
[9] C.A. Dyke, J.M. Tour, J. Am. Chem. Soc. 125 (2003) 1156–1157.
[10] C.A. Dyke, J.M. Tour, Nano Lett. 3 (2003) 1215–1218.
[11] M.A. Hamon, J. Chen, H. Hu, Y. Chen, M.E. Itkis, A.M. Rao, P.C. Eklund, R.C. Haddon, Adv. Mater. 11 (1999) 834–840.
[12] J. Bahr, J.M. Tour, J. Mater. Chem. 12 (2002) 1952–1958.
[13] S. Banerjee, T.H. Benny, S.S. Wong, Adv. Mater. 17 (2005) 17–29.
[14] Y.-P. Sun, K. Fu, Y. Lin, W. Huang, Acc. Chem. Res. 35 (2002) 1096–1104.
[15] K.A. Williams, P.T.M. Veenhuizen, B.G. de la Torre, R. Eritja, C. Dekker, Nature 420 (2002) 761.
[16] S. Ravindran, S. Chaudhary, B. Colburn, M. Ozkan, C.S. Ozkan, Nano Lett. 3 (2003) 447–453.
[17] S. Banerjee, S.S. Wong, J. Am. Chem. Soc. 125 (2003) 10342–10350.
[18] B. Azamian, K.S. Coleman, J.J. Davis, N. Hanson, M.L.H. Green, Chem. Commun. (2002) 366–367.
[19] S. Chaudhary, J.H. Kim, K.V. Singh, M. Ozkan, Nano Lett. 4 (2004) 2415–2419.
[20] J.M. Haremza, M.A. Hahn, T.D. Krauss, S. Chen, J. Calcines, Nano Lett. 2 (2002) 1253–1258.
[21] R.J. Chen, Y. Zhang, D. Wang, H. Dai, J. Am. Chem. Soc. 123 (2001) 3838–3839.
[22] A. Star, J.F. Stoddart, D. Steuerman, M. Diehl, A. Boukai, E.W. Wong, X. Yang, S.-W. Chung, H. Choi, J.R. Heath, Angew. Chem. Int. Ed. 40 (2001) 1721–1725.
[23] M. Zheng, A. Jagota, M.S. Strano, A.P. Santos, P. Barone, S.G. Chou, B.A. Diner, M.S. Dresselhaus, R.S. Mclean, G.B. Onoa, G.G. Samsonidze, E.D. Semke, M. Usrey, D.J. Walls, Science 302 (2003) 1545–1548.
[24] A. Satake, Y. Miyajima, Y. Kobuke, Chem. Mater. 17 (2005) 716–724.
[25] V. Biju, Y. Makita, A. Sonoda, H. Yokoyama, Y. Baba, M. Ishikawa, J. Phys. Chem. B 109 (2005) 13899–13905.
[26] Q. Shen, D. Arae, T. Toyoda, J. Photochem. Photobiol. A Chem. 164 (2004) 75–80.
[27] L.S.-H. Ichiya, B. Basner, I. Willner, Angew. Chem. Int. Ed. 44 (2005) 78–83.